Novel architecture of MEMS microphone with piezoresistive nano gauges detection

Jaroslaw Czarny, Emmanuel Redon, Thierry Verdot, Kerem Ege, Jean-Louis Guyader

NOVEL ARCHITECTURE OF MEMS MICROPHONE WITH PIEZORESISTIVE NANO GAUGES DETECTION

J. Czarny[1,2] , E. Redon[1*], T. Verdot[2], K. Ege[1] and J-L. Guyader[1]

[1] Laboratoire Vibrations Acoustique de l'INSA de Lyon,
25 bis, avenue Jean Capelle, 69621 VILLEURBANNE Cedex, FRANCE
Email: emmanuel.redon@insa-lyon.fr

[2] CEA-Leti, MEMS Sensors Laboratory
17, rue des Martyrs, 38054 GRENOBLE, FRANCE

ABSTRACT

Electret microphones dedicated to consumer electronics (mobile phone) and medical applications (hearing aids) have reached the miniaturization limits. Since the release of the first microphone based on silicon micromachining, electret microphones are constantly replaced by MEMS microphones. However, reduction of the diaphragm surface for MEMS is a fundamental limit to the miniaturization of microphones.

The following paper present a novel MEMS microphone architecture that is developed in the frame of the ANR MADNEMS project. It uses micro beams that deflect in the plane of the base wafer. Signal transduction is achieved by piezoresistive nanogauges integrated in the microsystem and attached to the micro beams. Acoustic pressure fluctuations lead to the deflection of the micro beams which produces a stress concentration in the nano gauges. Such architecture enables us to reduce the surface of the deflecting element and leads to a microphone with a smaller footprint that preserves at the same time high performances.

Accurate simulations based on the Finite Element Method of the discussed transducer couple acoustic, mechanical and electric behavior of the system. A 3D model of the microsystem would be too expensive in terms of computation time and memory with a poor mesh quality. This type of model is not suitable for the design of the MEMS microphone where numerous geometry parameters have to be revised. That is why a major effort has been devoted to modeling the microsystem by a 2D model. In particular, as the system is not symmetrical due to the deflection of the beams, a mechanical equivalent 2D model was proposed.

This paper presents the modeling approach used to taken into account mechanical and thermal boundary condition at the walls, and the phenomena of viscous and thermal diffusion involved in the air. Its implementation in a finite element code allows the numerical calculation of the pressure sensitivity of the microphone.

The numerical results were validated by an analytical model. The highlighting of the main physical phenomena in the microsystem, allowed to develop simplified models (Lumped Elements and Low Reduced Frequency) more suitable to the design of MEMS.

1 INTRODUCTION - ASSEMBLE OF THE MICROPHONE SUBSYSTEMS

Behavior (transfer function) of any microphone is a resultant of its acoustical, mechanical and electrical properties. Moreover in case of the MEMS microphones the acoustical properties are shaped by two subsystems: the properties of MEMS die and the properties of chip-scale package. To prepare reliable microphone model, one needs to investigate the inter-dependencies of this systems that are presented on Figure 1, therefore:

- acoustic system of the MEMS dice have three inputs (p_1, p_2 and q_m which are the pressure at the microphone input, the pressure in the backvolume and the flow generated by the movement of the mechanical structure relatively) and three outputs (q_1, q_2 and Δp which are the flow at the acoustic port of the microphone, flow entering the backvolume and the gradient of pressure established across the diaphragm respectively).
- The influence of the backvolume is coupled to the acoustic system by the feedback - the pressure p_2 is estimated with use of the flow rate q_2 that enters the backvolume.
- The mechanical system is coupled to the acoustic system with use of the pressure gradient Δp generated across the diaphragm. Mechanical system introduces to the acoustic system the flow rate q_m generated by the movement of the diaphragm.
  In case of our design the transduction is based on piezoresistive effect, thus the mechanical system is coupled to the electrical system by the stress σ_g generated inside the piezoresistors.
- Internal stress of a piezoresistor results in the variation of the resistance that is specified by the piezoresistive effect. Finally, the resistance variations may be interpret by Wheatstone bridge that is biased with current I_b and provided an output voltage ΔV.

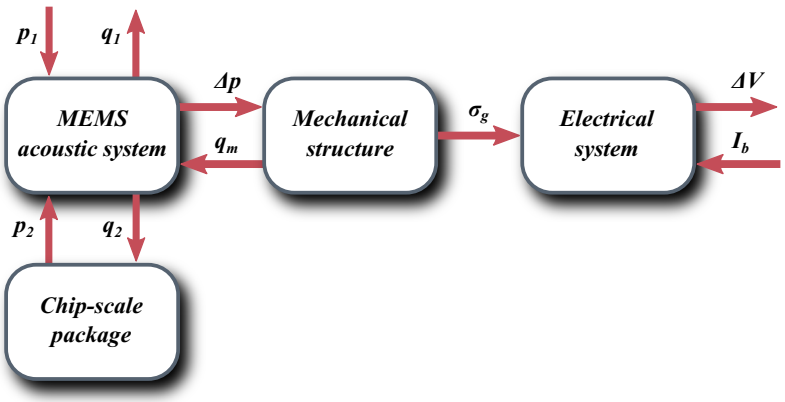

Figure 1: Transduction chain of a piezoresistive MEMS microphone.

2 SYSTEM ARCHITECTURE

New architecture of MEMS sensor that we propose in this paper is illustrated on Figure 2. It has overall dimensions of 1.5x1.5x0.6 mm^3, it consists of 4 micro-beams placed between the inlet vents that guide the sound waves and outlet vents connected to back cavity (Figure 3(a)). Dimensions of designed microphone ranges from 1 mm down to 1 µm. The smallest acoustic elements are the slits situated above and below the beam (Figure 3(b)). On the occurrence of sound, pressure

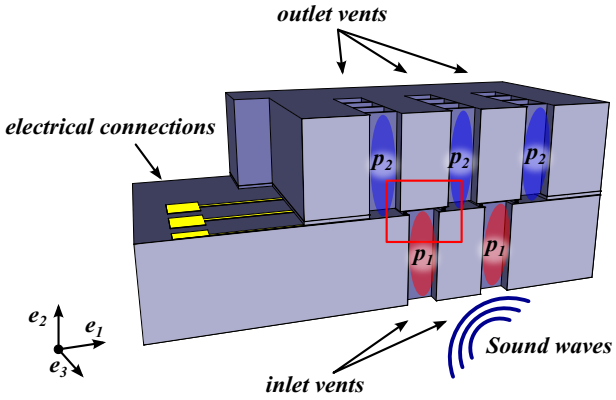

Figure 2: Cross-sectional scheme of the microphone with acoustic configuration and sensing elements.

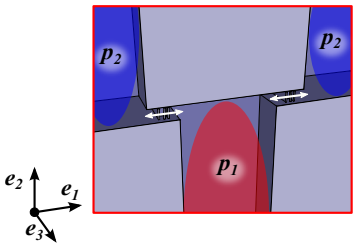

(a) Focus on two couplers. White arrows indicate position and in-plane displacement for two of four microstructures.

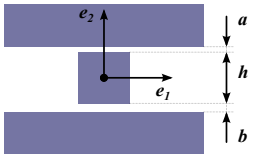

(b) Dimensions of a single coupler (not to scale).

fluctuations propagates through inlet vent and reach the diaphragm which deflects proportionally to the pressure difference between inlet and outlet vents ($\Delta p = p_1 - p_2$). Longitudinal stress induced by the motion of a beam inside suspended piezo resistive Si gauges is transduced into resistance variations and measured by use of full Wheatstone bridge architecture [1]. One side of each beam is attached to Si substrate through flexible hinge while the other side is free to ensure rotational movement (Figure 4).

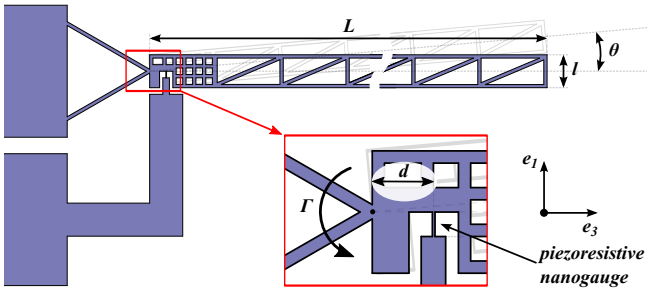

Figure 4: Top view and dimensions of single mechanical structure. Focus shows an arrangement of hinge and nanogauge.

3 TRUSS STRUCTURED BEAM - FROM 3D TO 2D SIMULATIONS

3D finite element model of fully-coupled microphone seems to be challenging in terms of computational cost. Therefore we pursued the 2D representation of the system which is not straightforward in case of acoustic properties of the coupler with the truss beam where the cross-sectional geometry vary across the e_3 direction (see Figure 4). The mechanical properties of the beam have been

lumped and introduced to the model with use of ordinary differential equations (these studies were already addressed in [2, 3]).

Acoustic investigations begun with 3D model where the 3D beam geometry was subtracted from the coupler geometry (no fluid-structure interaction). The aim of these models is to investigate only the acoustic properties, therefore to simplify the model we omit fluid-structure interaction and the beam outlines are simulated as the isothermal walls. Moreover in order to save the computation cost we model just one coupler, where the pressure at the inlet and outlet is set to 1 and 0 Pa. Even the 3D model of the coupler (without the fluid-structure interaction) that was used to extract the viscous resistance of the coupler is extremely expensive in terms of computation. To visualize the problematic of 3D simulations: properly meshed model that use COMSOL Thermoacoustic module takes 6 minutes to solve one frequency using 10 CPU's. During that time it solves the problem for over 5 millions DOF while using 100 GB of RAM. This extreme computation cost make 3D model inefficient for engineering problem which is the design of MEMS microphone where the numerous geometry parameters have to be revised.

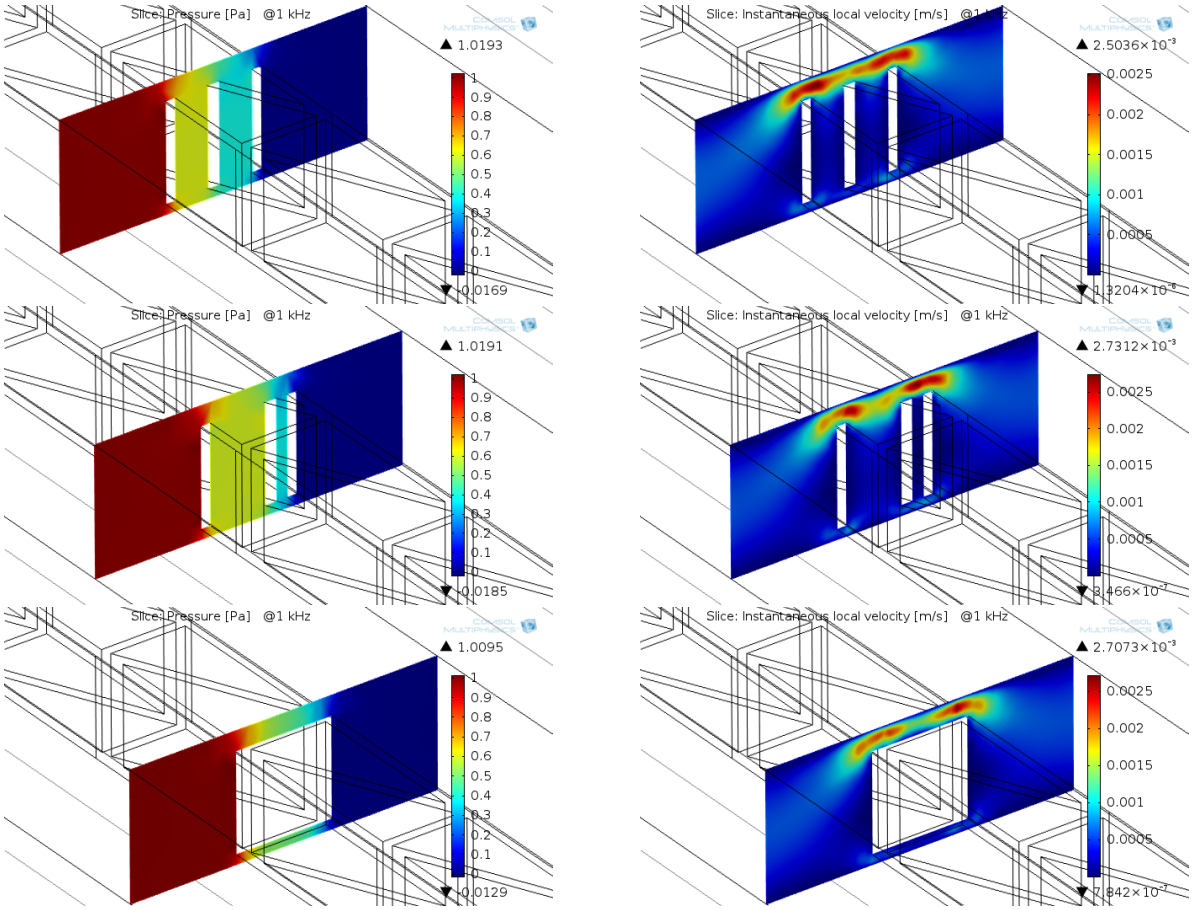

Figure 5: Pressure and velocity field distribution in 3D truss beam.

In order to prepare 2D model we face the acoustic problem which is the adjustment of viscous resistance introduced mainly by the gaps above and below the beam. To investigate this problem we have prepared three 2D models with different geometries of beam cross-sections:

first: truss is represented with rectangle where the width corresponds to the equivalent width calculated as a sum of truss members width (Figure 6),

second: truss is represented with rectangle where the width equals the overall with of truss beam l (Figure 7),

third: we represent the beam with three rectangles: two external where width equals the width of truss members and the central one which is slightly wider (1.2 µm) to take into account the angle of the central member of the truss (Figure 8).

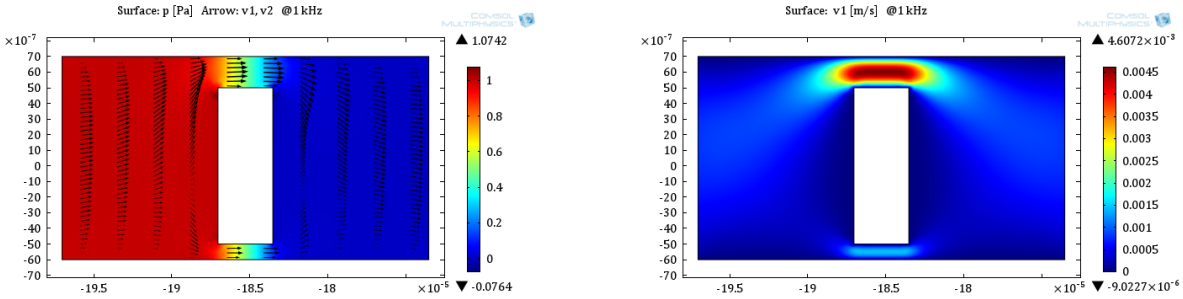

Figure 6: Truss beam represented with use the equivalent width.

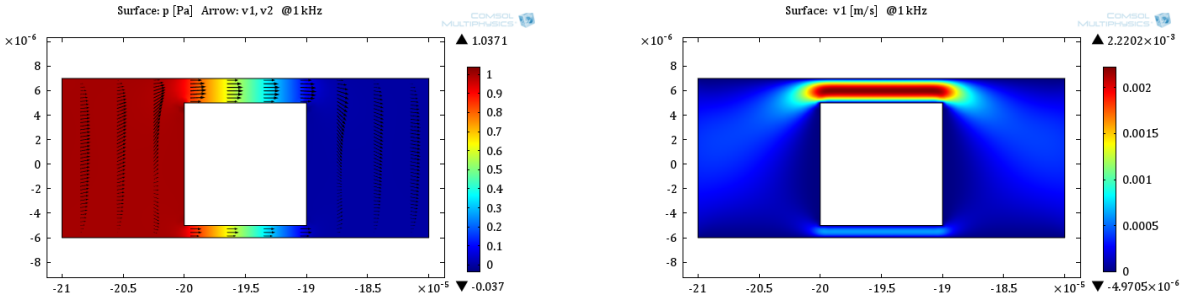

Figure 7: Truss beam represented with use the overall width.

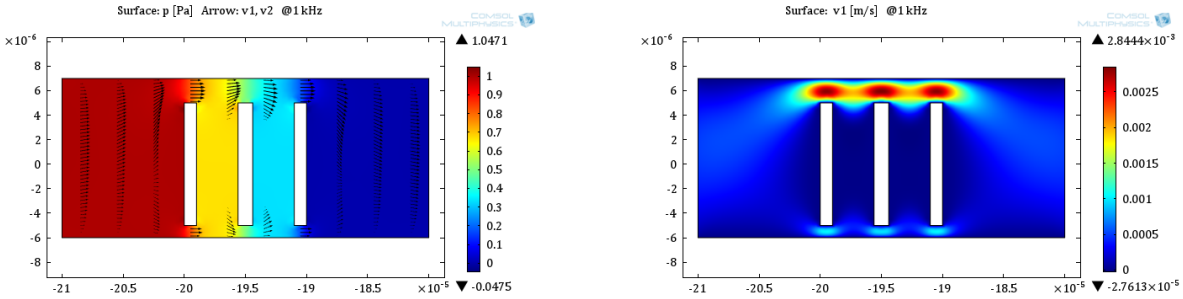

Figure 8: Truss beam represented with use of 2D "truss".

The resulting pressure and velocity fields for 1 kHz presented of Figures 6 - 8 are insufficient to compare the 2D modelisation approaches and appoint the most precise representation of 3D structure.

Therefore quantitative comparison of beam representation was made basing on the input admittance for the audible bandwidth (Figure 9). The admittance does not vary in audible range since the acoustic resonance of such small elements occurs at much higher frequencies. We may determine two extreme cases: geometry with equivalent width that has the lowest viscous resistance and the geometry with overall width that has the highest viscous resistance. We lean towards the intermediary solution which is the 2D "truss". This 2D representation slightly underestimates the input admittance of coupler with truss beam. This underestimation of the input admittance will generate the proportional error in estimation of the frequency response of the microphone (sensitivity). We accept this error and the further design procedure we use the 2D model with the beam represented as the 2D "truss".

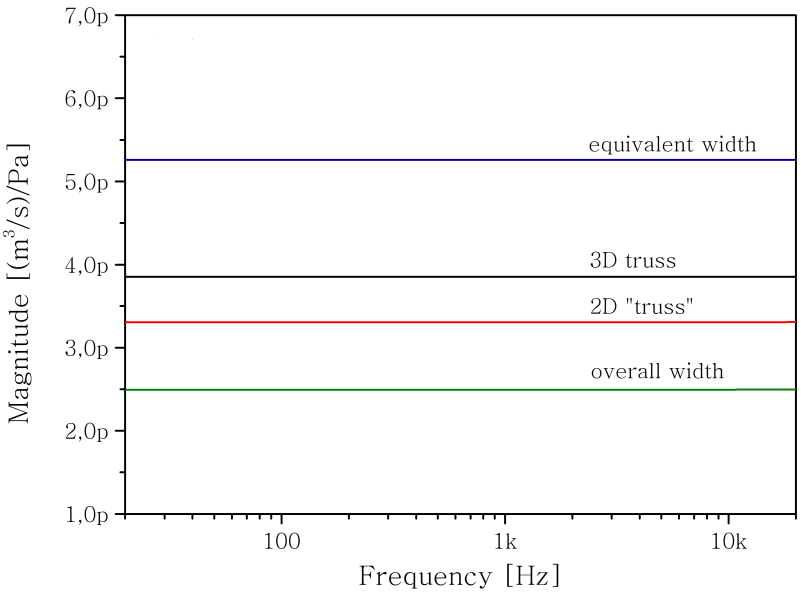

Figure 9: Comparison of input admittance for different 2D representations of truss beam.

4 2D FINITE ELEMENT ANALYSIS OF MEMS WITH FLUID-STRUCTURE INTERACTION

Dimensions of designed microphone ranges from 1 mm down to 1 µm. The smallest acoustic elements are the slits situated above and below the beam (Figure 3(b)). Their dimensions $a = 1$ µm and $b = 2$ µm are much smaller than the thicknesses of thermal and viscous boundary layers for the targeted sensor bandwidth (20Hz to 20kHz). Detailed analytical and FEM models that investigates thermoviscous effects have been prepared within the M&NEMS microphone project and presented by C. Guianvarc'h and T. Verdot [2, 3]. Using a simplify model for moving beams, these models handle fluid-structure interactions.

4.1 Acoustic and thermal boundary conditions

We present the cross-section of the MEMS chip on Figure 10 with the boundary conditions that are required to meet the acoustic and mechanical behavior of the device. Therefore the surfaces of

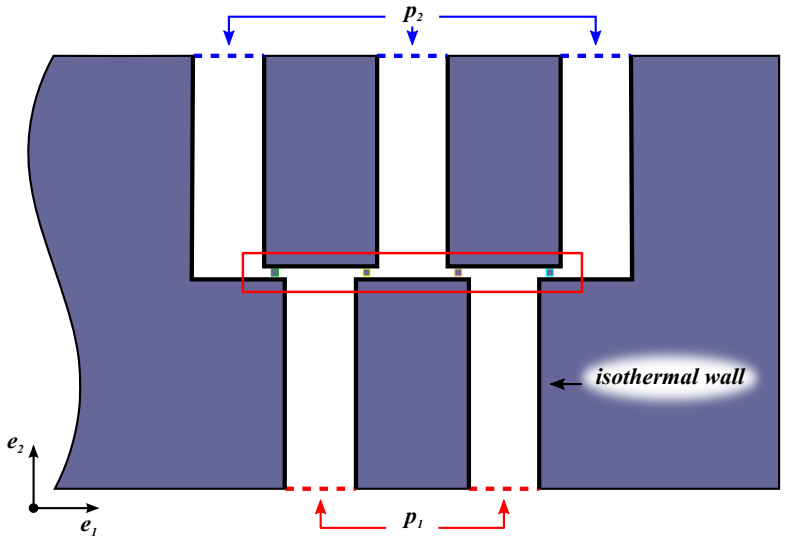

Figure 10: Cross-sectional view of MEMS with boundary conditions indicated.

the acoustic system are simulated as the isothermal wall (non-slip conditions and no temperature variations); we impose the pressure p_1 at the MEMS inlet and p_2 at the MEMS outlet.

4.2 Fluid-Structure Interaction (FSI)

Closer look on the couplers, where the fluid-structure interaction is realized is presented on the Figure 11. The velocity of the fluid and the beams on the fluid-structure interface (the countour of

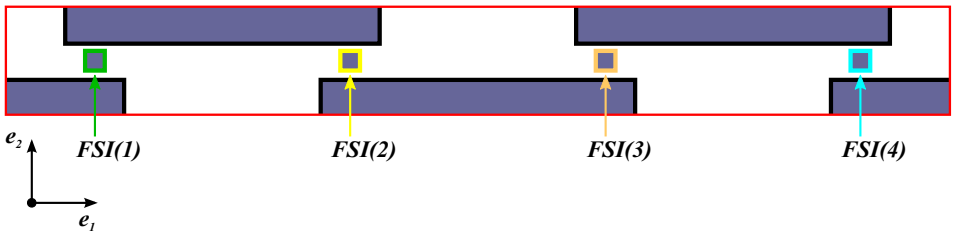

Figure 11: Closer view on the ”couplers”.

the beam) is set to be equal:

$$\frac{L}{2}\dot{\theta} - \mathbf{v} = 0 \tag{1}$$

and it is a resultant of the beam movement driven by the acoustic pressure fluctuations where both mechanical and acoustical problems are solved independently. The mechanical behavior of the beams is governed by the analytical model and introduced into the FEM with use of ordinary differential equations. The displacement of the beams in 2D model is approximated by the average displacement of the rotating beam (Figure 12).

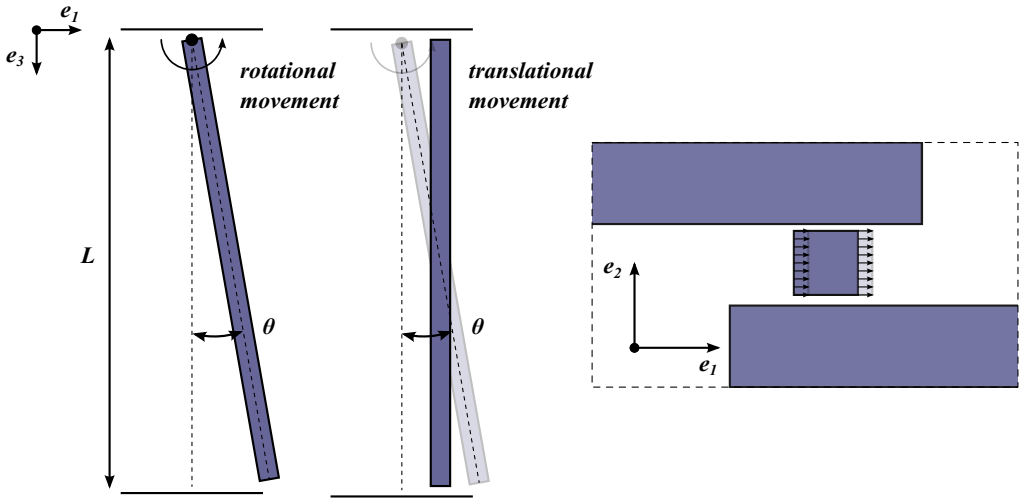

Figure 12: Representation of rotationall movement of the beam in 2D.

4.3 Influence of MEMS chip-scale packaging on the microphone response

Typical chip-scale MEMS microphone package showed on Figure 13 includes two separated chips which are MEMS and ASIC (Application-Specific Integrated Circuit). To calculate the frequency response of the microphone, we must obviously take into account the volume called the back-volume (obtained by deducting the volumes of the MEMS and the ASIC chips from the internal volume of a package). The backvolume (V_{ar}) introduces acoustic compliance C_{ar}:

$$C_{ar} = \frac{V_{ar}}{\gamma P_0}, \tag{2}$$

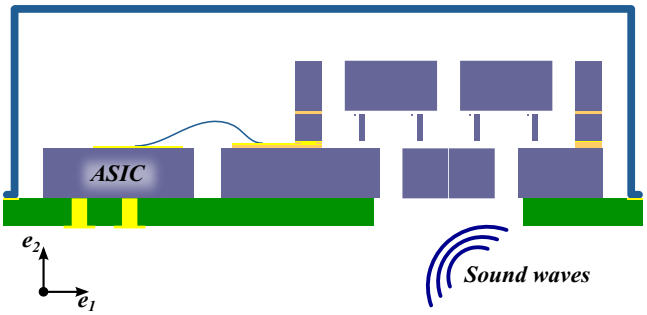

Figure 13: Bottom port configuration of MEMS microphone package (not to scale).

where γ denotes ratio of specific heats for air and P_0 is the static pressure. Regarding the closed cavity of package with dimensions larger than thermal and viscous boundary layers we can use the law of mass conservation:

$$\int_{V_{ar}} \frac{\mathrm{d}V}{\gamma P_0} \frac{\partial p_{ar}}{\partial t} = \int_{V_{ar}} -\nabla \cdot v \, \mathrm{d}V, \tag{3}$$

where p_{ar} is a pressure in backvolume and it equals p_2. By solving the integrals from equation 3 we obtain the time derivative of pressure inside the backvolume that can be implemented in FEM as an ordinary differential equation:

$$\frac{\partial p_{ar}}{\partial t} = \frac{q_{ar}}{C_{ar}}, \tag{4}$$

where q_{ar} is a total volumetric flow entering the backvolume and it equals q_2.

5 EQUIVALENT CIRCUIT REPRESENTATION OF THE MICROPHONE

Equivalent circuit representation is a popular technique of MEMS microphones simulations. It has been applied by several authors [4–8] to model MEMS microphones response and the noise budget. Moreover it seems to be the most convenient method to estimate the output noise generated by the system. For sake of simplicity, we present the lumped elements of the designed microphone on the example of one beam (Figure 14).

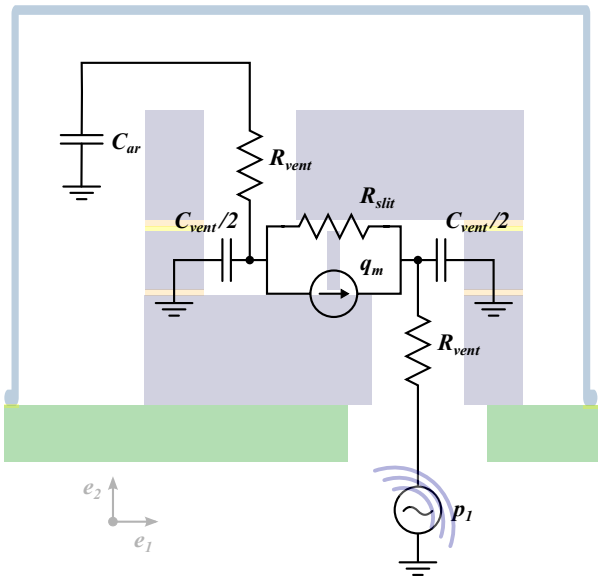

Figure 14: Lumped elements of the microphone presented on single coupler.

We may then identify the following elements:

- p_1 is the acoustic pressure at the input of the microphone,
- R_{vent} is the viscous resistance of the inlet and outlet vents,
- C_{vent} is the acoustic compliance of the inlet and outlet vents,
- R_{slit} is the combined viscous resistance of the gaps above and below the beam,
- q_m is the air flow generated by the mechanical structure,
- C_{ar} is the acoustic compliance of the backvolume.

If we want to represent the full architecture of designed microphone, we need to take four beams, two inlet vents and three outlet vents. The microphone simulations based on such circuit may be done in Spice software or by use of Linear Time-Invariant (LTI) models in MATLAB.

Our considerations assume that the air is non compressible in the slits above and below the beams. Moreover for audible bandwidth inertial effects can be neglected. Including viscous shear stress in the air μ, Navier-Stokes momentum balance equation provides relationship between the pressure p and velocity $\mathbf{v}$ fields [9]:

$$\frac{\partial p}{\partial x} = \mu \frac{\partial^2 \mathbf{v}}{\partial y^2}, \tag{5}$$

Equation 5 is integrated considering difference of pressure across the coupler Δp and no-slip conditions at fluid-structure interfaces. As a result we obtain formula for volumetric air flow inside the coupler q_c:

$$q_c = \frac{1}{R_{slit}} \Delta p + \frac{L}{2} S_d^* \dot{\theta}, \tag{6}$$

where $\dot{\theta}$ is the angular velocity of the beam (see Figure 4), R_{slit} denotes the total viscous resistance of gaps that is calculated with LRF model and given later and S_d^* is modified lateral surface of a beam driven by viscous effects:

$$S_d^* = (Lh) \left(1 + \frac{a+b}{2h} \right). \tag{7}$$

The second part of equation 6 is the air flow generated by the mechanical structure:

$$q_m = \frac{L}{2} S_d^* \dot{\theta}. \tag{8}$$

Torque applied to rotating beam is defined by acoustic force reduced by viscous shear damping:

$$\Gamma_A = \frac{L}{2} S_d^* \Delta p - D_V \dot{\theta}, \tag{9}$$

where viscous shear damping lumped coefficient D_V is:

$$D_V = \frac{\mu L^2}{3} (lL) \left(\frac{1}{a} + \frac{1}{b} \right). \tag{10}$$

The acoustic compliance of the backvolume is calculated with use of the following formula:

$$C_{ar} = \frac{V_{ar}}{\gamma P_0}. \tag{11}$$

In this model the values of some elements are designated with use of the LRF model approach (see the work of W.M. Beltman [10] and R. Kampinga [11] for further details). With this approach we have determined the value of R_{slit}, R_{vent} and C_{vent}:

Symbol	Value	Unit
R_{slit}	3.2444e11	$[Pa/(m^3 s)]$
R_{vent}	9.987e7	$[Pa/(m^3 s)]$
C_{vent}	3.59e-19	$[m^3/Pa]$

Table 1: Lumped elements determined with use of LRF model.

6 SENSITIVITY

Total sensitivity of a microphone is the assembly of its acoustical, mechanical and electrical transfer functions. The sensitivity response given in this section is designated with use of three different models:

- 2D FEM model,
- simplified 3D FEM model,
- Lumped Element Model.

3D model is not an efficient tool for the design of M&NEMS microphone and the value of the sensitivity has been calculated only for 1 kHz. It was prepared in order to estimate the error introduced by the 2D representation. We have prepared the fully-coupled 3D model in which we have limited the microphone geometry to one coupler and the beam. We have set the gradient of pressure across the coupler to 1 Pa at the frequency of 1 kHz (Figure 15(a)). The estimation of the average stress generated inside the nanogauge (Figure 15(b)) lead us to the value of the sensitivity which is compared to the one obtained with 2D model.

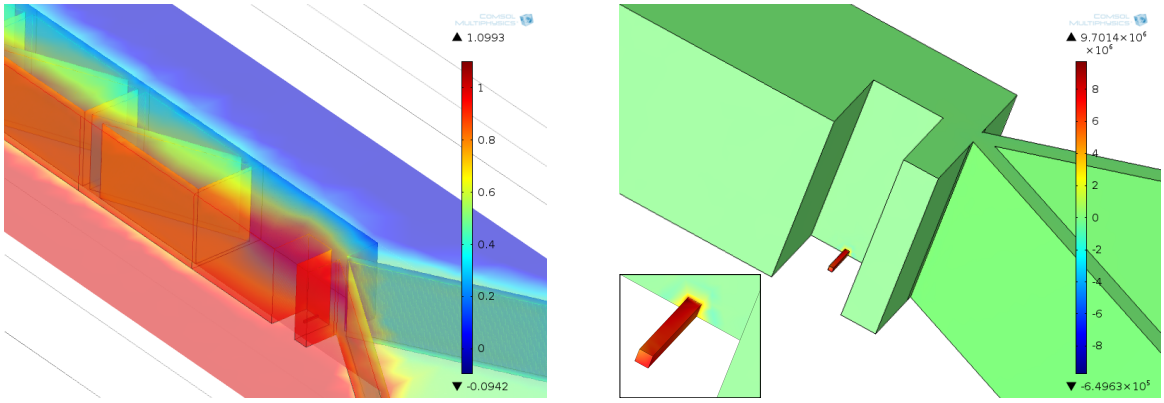

(a) Pressure field distribution.

(b) Stress accumulation inside the nanogauge.

Figure 15: 3D model of one coupler and the beam with fluid-structure interaction.

Two remaining models give nearly similar response for the whole bandwidth (Figure 16). In these models the mechanical behavior of the beam is governed with the same analytical approach, however the acoustic phenomena model differs and it is more precise in case of FEM. This difference is visible at low frequency and at the resonant frequency. It is mainly caused by different way of viscous resistance estimation.

For the purpose of sensitivity analysis we have prepared the general equation that describes the sensitivity, however we need to remember that such elements as: S_d^*, Q_V and τ_{RC} are designated in different manner for each model. The components that do not depend on the frequency are gathered and expressed as S_0, the nominal sensitivity of a microphone:

$$S_0 = [\pi_{pzr} V_b] \left[\frac{S_d^*}{S_g}\right] \left[\frac{L/2}{d}\right] \frac{dK_g d}{C_h + dK_g d}. \tag{12}$$

Then, to obtain the total sensitivity we add the terms that depends on the frequency:

$$S(\omega) = \frac{\Delta V}{p_1} = S_0 \left[\frac{1}{1 - \left(\frac{\omega}{\omega_0}\right)^2 + \frac{1}{Q_V}\left(j\frac{\omega}{\omega_0}\right)} \right] \left[\frac{\tau_{RC} j\omega}{1 + \tau_{RC} j\omega} \right]. \tag{13}$$

Lower limit of a microphone bandwidth is fixed by the inverse of time constant $1/\tau_{RC}$ coming from viscous resistance of the slits and the acoustic compliance of the back volume. High frequency limit is set by the first mechanical resonance frequency of M&NEMS structure.
Nominal sensitivity at $f = 1$ kHz and bias voltage of Wheatstone bridge $V_b = 0.46$ V is estimated with 2D FEM simulations to -56.4 dBV (1.5 mV/Pa). This value is an output voltage of Wheatstone bridge, the final sensitivity of the microphone will be enlarged by amplification of readout electronics (ASIC).

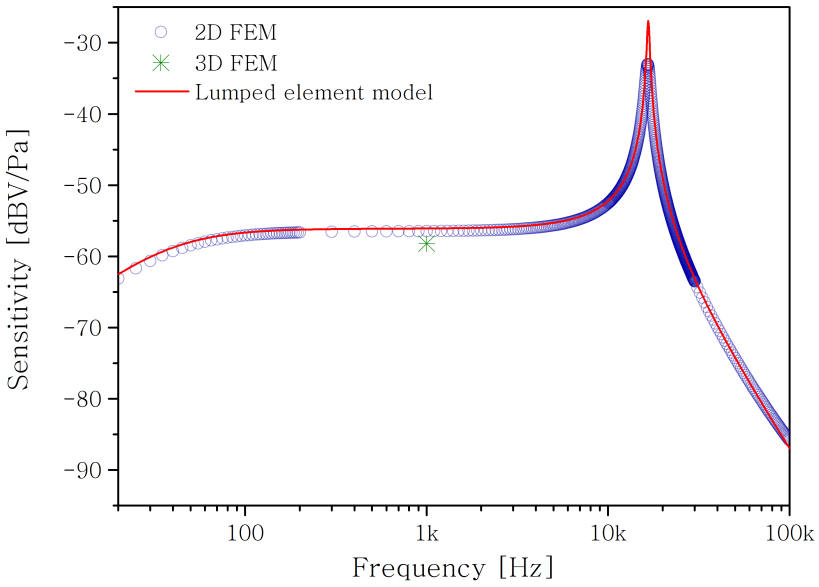

Figure 16: Frequency response of the MADNEMS microphone.

7 CONCLUSION

ACKNOWLEDGMENTS

This work was performed within the framework of the Labex CeLyA of Universit de Lyon, operated by the French National Research Agency (ANR-10-LABX-0060/ ANR-11-IDEX-0007).
Development of M&NEMS microphone is supported by the French National Research Agency (MADNEMS project ANR11-NANO-026).

REFERENCES

[1] W. Kester. Practical design techniques for sensor signal conditioning. Analog Devices Technical Reference Books, 1999.

[2] C. Guianvarc'h, T. Verdot, J. Czarny, E. Redon, K. Ege, J.-L. Guyader, A. Walther, and P. Robert. New planar nano-gauge detection microphone: analytical and numerical acoustic modeling. *Proceedings of Meetings on Acoustics*, 19(1):–, 2013.

[3] T. Verdot, C. Guianvarc'h, J. Czarny, E. Redon, K. Ege, and J.L. Guyader. Modélisation d'une architecture innovante de microphone MEMS à détection par nano jauges. In *Actes du XXIe Congrès Français de Mécanique, CFM2013*, Bordeaux, France, 2013.

[4] A. Dehe, M. Wurzer, M. Fuldner, and U. Krumbein. The Infineon silicon MEMS microphone. In *Proceedings SENSOR 2013*, pages 95–99, 2013.

[5] J.J. Neumann Jr. and K.J. Gabriel. A fully-integrated CMOS-MEMS audio microphone. In *TRANSDUCERS, Solid-State Sensors, Actuators and Microsystems, 12th International Conference on, 2003*, volume 1, pages 230–233, 2003.

[6] M. Sheplak, J.M. Seiner, K.S. Breuer, and M.A. Schmidt. A MEMS microphone for aeroacoustics measurements. In *37th AIAA Aerospace Sciences Meeting & Exhibit, AIAA Paper 99-0606*, Reno, NV, January 1999.

[7] M.L. Kuntzman, C.T. Garcia, A.G. Onaran, B. Avenson, K.D. Kirk, and N.A. Hall. Performance and modeling of a fully packaged micromachined optical microphone. *Microelectromechanical Systems, Journal of*, 20(4):828–833, 2011.

[8] M.D. Williams, B.A. Griffin, T.N. Reagan, J.R. Underbrink, and M. Sheplak. An AlN MEMS piezoelectric microphone for aeroacoustic applications. *Microelectromechanical Systems, Journal of*, 21(2):270–283, 2012.

[9] P.Y. Kwok, M.S. Weinberg, and K.S. Breuer. Fluid effects in vibrating micromachined structures. *Microelectromechanical Systems, Journal of*, 14(4):770–781, Aug 2005.

[10] W.M. Beltman. Viscothermal wave propagation including acousto-elastic interaction, part I: Theory. *Journal of Sound and Vibration*, 227(3):555 – 586, 1999.

[11] W.R. Kampinga. *Viscothermal acoustics using finite elements : analysis tools for engineers*. PhD thesis, Enschede, June 2010.